JACS
JOURNAL OF THE AMERICAN CHEMICAL SOCIETY

Communication

pubs.acs.org/JACS

Direction Control of Oriented Self-Assembly for 1D, 2D, and 3D Microarrays of Anisotropic Rectangular Nanoblocks

Yoshitaka Nakagawa, Hiroyuki Kageyama, Yuya Oaki, and Hiroaki Imai*

Department of Applied Chemistry, Faculty of Science and Technology, Keio University, 3-14-1 Hiyoshi, Kohoku-ku, Yokohama 223-8522, Japan

Supporting Information

ABSTRACT: Micrometric linear chains (1D arrays), monolayers (2D arrays), and superstructures (3D arrays) of anisotropic Mn_3O_4 nanocuboids were selectively produced by oriented self-assembly through evaporation of a dispersion. The 1D arrays were basically formed on a substrate via oriented self-assembly of the rectangular crystals in the ⟨100⟩ direction. The 2D and 3D microarrays were obtained by adjusting the particle concentration of the dispersion. The [001] direction of tetragonal crystal was controlled to be parallel and perpendicular to the substrate by changing the polarity of the medium.

Self-assembly of nanometric building blocks is a fascinating phenomenon as a bottom-up approach to achieving a wide range of novel functional materials with ordered architectures. 2D and 3D close-packed arrays of uniform spherical nanoparticles are built through self-assembly in liquid media.[1,2] Various types of mesoscale unit cells are produced with different-sized binary or ternary nanospheres.[3−5] In the ordered arrays, the crystallographic direction of the building units is regulated with oriented self-assembly of specific crystal lattices or the accumulation of rectangular blocks, especially nanocubes synthesized from various cubic crystals, including metals and metal oxides.[6−19] 2D and 3D single-crystal-like superlattices are formed via self-assembly of the nanocubes in the same crystallographic orientation.[8,9,11,12,20] Micrometer- to millimeter-scale assemblies of the nanoblocks have been fabricated on a substrate by convective self-assembly using dispersion.[21−24] Highly ordered assemblies of nanoparticles are obtained through the lateral capillary force between neighboring particles when the liquid evaporates. A wide variety of supercrystals, 3D superlattices having well-defined micrometric facets, are constructed via 3D assembly of nanocubes.[7,8,13−16,25] Although the macroscopic morphology of the supercrystals is changed by the shape of the nanocrystals,[16] the supercrystals exhibit isotropic morphologies due to the isotropic shapes of the nanoscale units. Recently, control of the crystallographic direction for 1D and 2D arrays has been achieved by using truncated nanocubes.[26] Anisotropic shaped superstructures, such as linear chains, are fabricated with anisotropic blocks.[27−29] However, regulation of the direction and dimension of the oriented self-assembly is fundamentally difficult without any external fields. The crystallographic orientations of 1D, 2D, and 3D ordered arrays have not been sufficiently controlled for the fabrication of assemblies with diverse shapes.

In the present work, direction control of oriented self-assembly for 1D, 2D, and 3D microarrays is achieved using anisotropic nanocuboids as building blocks. We demonstrate the ordered assembly of tetragonal Mn_3O_4 covered with oleic acid by a convective self-assembly method as shown in Figure S1a. Synthesis of the metal oxide nanoblocks and control of their assembly are very significant for practical use in technological applications[15,25] because of their potential as active catalysts,[30,31] magnetic materials,[32] and electrode materials[33−37] for rechargeable lithium-ion batteries.[34−37] Here, the accumulation process of the Mn_3O_4 rectangular nanoblocks was controlled by the conditions of the dispersion as shown in Scheme 1. Linear chains and two types of

Scheme 1. Direction Control of Oriented Self-Assembly for 1D, 2D, and 3D Microarrays of Anisotropic Rectangular Nanoblocks by Changing Dispersion Media and Particle Concentration

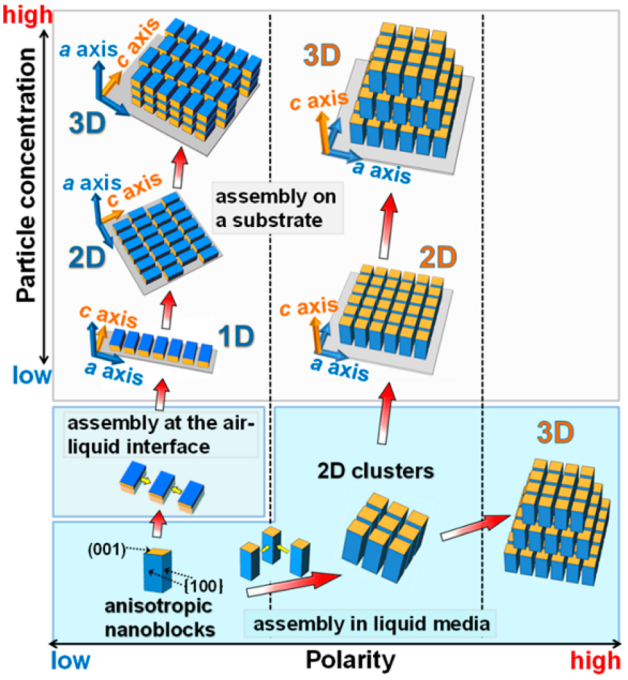

Received: October 3, 2013
Published: December 27, 2013

   dx.doi.org/10.1021/ja410183q | J. Am. Chem. Soc. 2014, 136, 3716−3719

monolayers and superlattices with different crystallographic directions were fabricated by changing the particle concentration and the polarity of the dispersion medium.

As shown in Figure 1, anisotropic rectangular nanoblocks were synthesized through a two-phase (water and toluene)

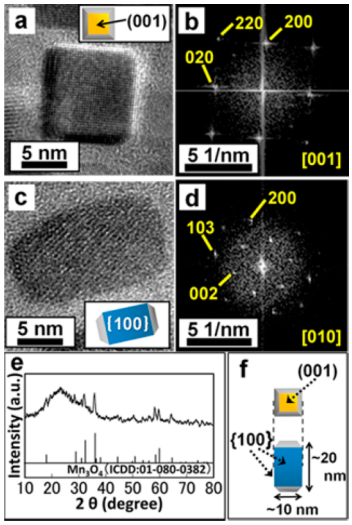

Figure 1. HRTEM images and FFT patterns corresponding to the lattice fringes of Mn_3O_4 rectangular nanoblocks with a projection direction of [001] (a,b) and [100] (c,d). XRD pattern of the product (a broad halo at 20−30° is ascribed to a glass holder) (e). Schematic illustration of a standard Mn_3O_4 rectangular nanoblock (f).

solvothermal method containing oleic acid and *tert*-butylamine. The X-ray diffraction (XRD) peaks (Figure 1e) and fast Fourier transform (FFT) spots corresponding to the lattice fringes (Figure 1a−d) of the nanocrystals were assigned to tetragonal Mn_3O_4 (a = 0.576 nm and c = 0.947 nm). The resultant nanocuboids exhibit truncated cuboids with four definite {100} faces (Figure 1a,c). The width and length of the cuboids produced under the standard condition were ∼10 and ∼20 nm, respectively (Figure 1f). The particle size increased by increasing the amounts of the manganese sources, oleic acid, and *tert*-butylamine, whereas the aspect ratio was almost fixed (Figure S2). According to the thermogravimetry analysis, the resultant rectangular nanoblocks were covered with ∼14 wt% of organic components (Figure S3). The nucleation was deduced to have occurred in the water phase near the liquid−liquid interface with an increase in the pH value through hydrolysis of *tert*-butylamine above 100 °C. The rectangular blocks coated with oleic acid were then formed in the toluene phase.[6]

As shown in Figure 2, we observed alignments of several nanocuboids of Mn_3O_4 on a collodion film after evaporation of the dispersion medium. The interparticle distance (3.2 nm) is close to twice the molecular length of oleic acid (1.7 nm; Figure 2b). This suggests that the nanoblocks were covered with the molecules that were slightly tilted.[20] A set of the FFT patterns of lattice fringes (Figure 2c) was obtained from the three adjacent nanocuboids. This indicates that the nanoblocks were strictly arranged in the same crystallographic orientation. The Mn_3O_4 cuboids tend to be aligned in the ⟨100⟩ direction when rectangular faces, as opposed to square faces, are attached (Figure 2d). Because the surface area of the rectangular faces is larger than that of the square faces, the contacts of the rectangular sides are more effective for decreasing the total

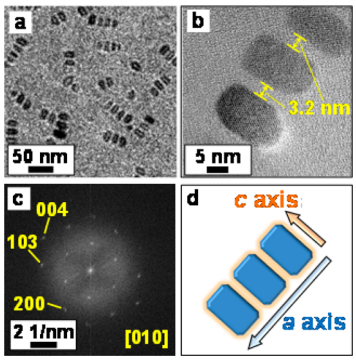

Figure 2. TEM image of aligned Mn_3O_4 rectangular nanoblocks (a). HRTEM image of three adjacent Mn_3O_4 nanocuboids and their FFT patterns (b,c). Schematic illustration of three adjacent Mn_3O_4 nanocuboids (d).

surface energy of the assemblies than are those of the square sides.

We accumulated the Mn_3O_4 rectangular nanoblocks on a silicon substrate using a convective self-assembly method. The assembled architectures could be controlled by changing the particle concentration and the dispersion medium (Scheme 1). Linear chains (1D arrays) of the cuboids were obtained from the dispersion of a mixture of hexane and toluene (1:1 in volume) at a low particle concentration (2.2×10^{-3} g/dm^3) (Figure 3a,b). Chains approximately 200−1000 nm in length

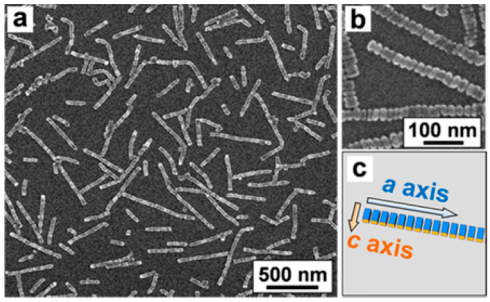

Figure 3. SEM images (a,b) and schematic illustration (c) of linear chains consisting of Mn_3O_4 rectangular nanoblocks aligned in the ⟨100⟩ direction.

were composed of 10−50 nanoblocks. Because we observed large {100} faces as shown in Figure 3b, the linear chains consisted of nanoblocks aligned in the ⟨100⟩ direction (Figure 3c). Since the chains were gradually aggregated through a slow evaporation at room temperature, rapid evaporation by heating on a hot plate was effective for the production of isolated chains on the substrate.

Monolayers (2D arrays) of the Mn_3O_4 nanocuboids were fabricated by increasing the particle concentration to 2.8×10^{-1} g/dm^3 (Figure 4a−d). The dispersion medium was slowly evaporated at room temperature to promote parallel assembly of the linear chains. Because the substrate was observed in void spaces of the arrays (Figure 4d), a monolayer arrangement is suggested. The FFT spots (Figure 4a inset) indicate that the ordered 2D arrays consist of linear chains approximately 30 nm in width. Because the periodicity corresponds to the length of the nanocuboid in the direction of the long axis, the linear chains are deduced to align in the [001] direction in the arrays. On the other hand, FFT spots in the ⟨100⟩ direction were not observed. This suggests that nanoblocks in the linear chains are

dx.doi.org/10.1021/ja410183q | J. Am. Chem. Soc. 2014, 136, 3716−3719

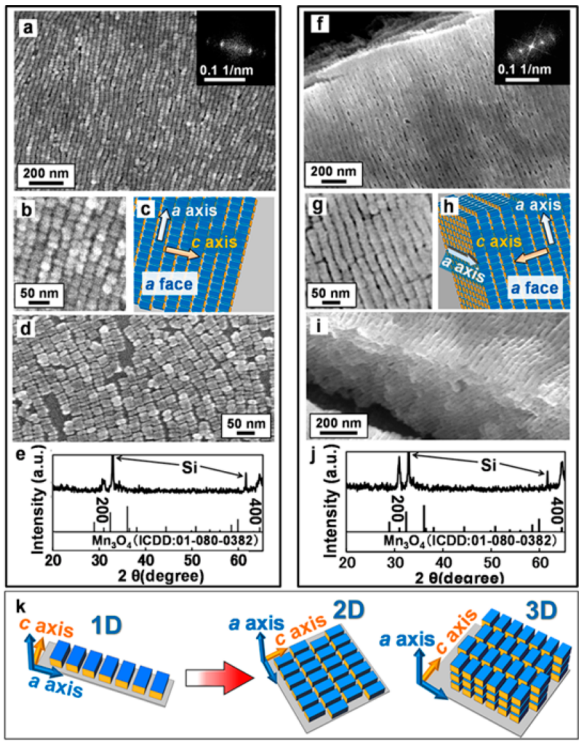

Figure 4. 2D and 3D arrays with a {100} face parallel to the substrate: SEM images and the corresponding FFT pattern (inset) and schematic illustration of 2D arrays (a–d). XRD pattern of 2D arrays on a silicon substrate (e). SEM images and the corresponding FFT pattern (inset) and schematic illustration of 3D arrays (f–h). SEM image of the cross-section of 3D arrays (i). XRD pattern of 3D arrays on a silicon substrate (j). Schematic illustration of the formation of 2D and 3D arrays through parallel assembly of 1D chains (k).

displaced by a half unit in the ⟨100⟩ direction (Figure 4k). Superlattices (3D arrays) of the nanocuboids were obtained by increasing the concentration to 5.6×10^{-1} g/dm^3 (Figure 4f–i). The 3D arrays were confirmed to consist of more than 10 layers of 2D arrays according to the same FFT pattern as that of the 2D arrays (Figure 4f inset) and an SEM image (Figure 4i). Because intense (200) and (400) peaks were observed in the XRD pattern (Figure 4e,j), the {100} plane was parallel to the substrate in the 2D and 3D arrays. The size of the ordered domains was 2–5 μm^2. The 2D and 3D arrays exposing the {100} face are produced by parallel assembly of the linear chains (Figure 4k).

Figure 5 shows another type of 2D array obtained on the substrate using a dispersion of toluene through gentle evaporation at room temperature. Arrangements of the square sides of nanocuboids in a square grid pattern were observed. This suggests that the (001) plane is parallel to the substrate in the arrays (Figure 5a–c). The FFT pattern supports the tetragonal arrangement of quadrate units of 20 nm in size (Figure 5a inset). Through observation of their edges, we confirmed that the arrays are monolayers (Figure 5d). The size of the ordered domains was approximately 1 μm^2. The 3D arrays in the square grid pattern that were 2–5 μm wide were produced by increasing the particle concentration to 5.6×10^{-1} g/dm^3 (Figure 5e–g). Two- or three-layered structures were obtained on the collodion film from the dispersion (Figure 5h). The SAED image of the multilayers indicates that the [001] direction of the 3D microarrays is perpendicular to the substrate (Figure 5i). We found 2D clusters consisting of 4–

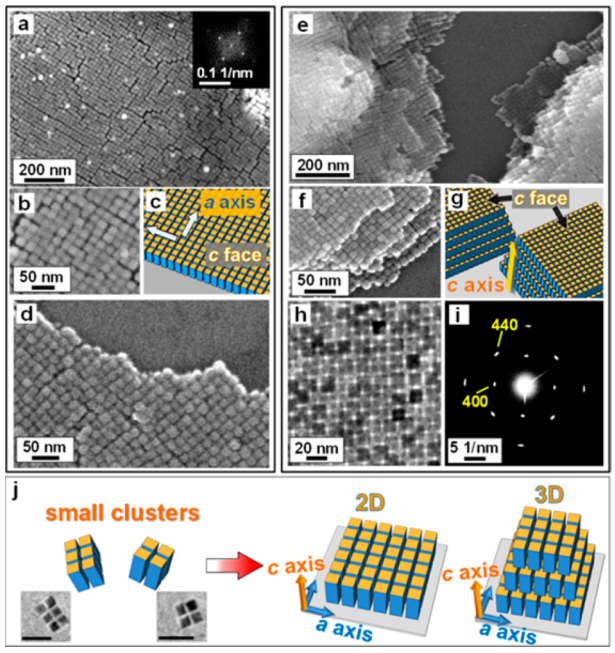

Figure 5. 2D and 3D arrays with a (001) face parallel to the substrate: SEM images and the corresponding FFT pattern (inset) and schematic illustration of 2D arrays produced on a silicon substrate (a–d). SEM images and schematic illustration of 3D arrays (e–g). TEM image of 3D arrays and its SAED pattern (h,i). Schematic illustration of the formation of 2D and 3D arrays through oriented self-assembly of small clusters and TEM images of the 2D clusters (scale bars are 50 nm) (j).

6 nanocuboids that were arranged in two ⟨100⟩ directions (TEM images in Figure 5j). Thus, we deduced that the 2D and 3D arrays are formed on the substrate through the accumulation of small clusters by evaporation.

3D superlattices approximately 4 μm wide were observed on the silicon substrate even at a low concentration (2.2×10^{-3} g/dm^3), when ethanol was used as a dispersion medium (Figure 6). The size of the quadrate units (20 nm) calculated from the FFT spots of the 3D arrays indicates that the (001) face of the nanocuboids is parallel to the substrate (Figure 6a–c). We also

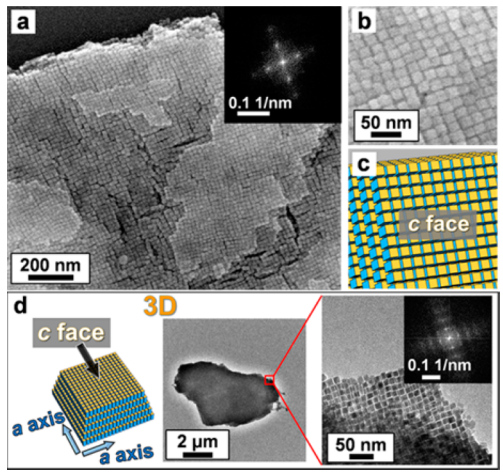

Figure 6. 3D arrays with a (001) face parallel to the substrate: SEM images, the corresponding FFT pattern (inset), and schematic illustration of 3D arrays (a–c). Schematic illustration and TEM images of 3D arrays formed in ethanol and the corresponding FFT pattern (inset) (d).

dx.doi.org/10.1021/ja410183q | J. Am. Chem. Soc. 2014, 136, 3716–3719

found 3D arrays on the collodion film when ethanol was evaporated (Figure 6d). This result suggests that 3D arrays are directly formed in ethanol.

Basically, the anisotropic nanocuboids of Mn_3O_4 are aligned in the ⟨100⟩ directions of the tetragonal crystal (Figure 2). We deduced that 1D arrays are formed at the air−liquid interface by lateral capillary force when the medium is evaporated, as reported in previous works (Figure 3).[20,28] 2D and 3D arrays that expose the {100} face are produced by parallel assembly of the linear chains when the particle concentration is increased (Figures 4 and S1b). The hydrophobic nanocuboids covered with oleic acid aggregate when the polar character of the medium is increased. Thus, small 2D clusters of nanocuboids arranged in two ⟨100⟩ directions are formed in toluene. The micrometric 2D and 3D arrays that expose the (001) face are obtained through accumulation of the clusters on the substrate (Figures 5 and S1c). The 3D arrays are directly formed though assembly of the clusters in ethanol, even at a low particle concentration (Figure 6). The specific formation mechanisms are discussed in the Supporting Information (Figure S1).

In summary, micrometric 1D, 2D, and 3D ordered arrays of nanoblocks were selectively produced on a substrate through self-assembly of anisotropic Mn_3O_4 nanoblocks. Linear chains (1D arrays) elongated in the ⟨100⟩ direction of the tetragonal crystal were produced on a substrate from highly dispersed nanocuboids through evaporation of a hydrophobic medium. Monolayers (2D arrays) and superlattices (3D arrays), consisting of nanocuboids with a {100} face that was parallel to the substrate, were produced by increasing the particle concentration to stack the linear chains. Another type of arrays, having the (001) face parallel to the substrate, was obtained by assembling the 2D clusters with increased polarity of the medium. The anisotropic shape of the building blocks is essential for controlling the crystallographic orientation of the various dimensional assemblies. This direction- and dimension-controlled self-assembly process is regarded as a novel fabrication technique for a wide variety of functional nanomaterials.

■ ASSOCIATED CONTENT

Ⓢ Supporting Information

Experimental procedure and additional information and data. This material is available free of charge via the Internet at http://pubs.acs.org.

■ AUTHOR INFORMATION

Corresponding Author

hiroaki@applc.keio.ac.jp

Notes

The authors declare no competing financial interest.

■ ACKNOWLEDGMENTS

This work was supported by the Advanced Low Carbon Technology Research and Development Program (ALCA) from Japan Science and Technology Agency (JST), Japan.

■ REFERENCES

(1) Bigioni, T. P.; Lin, X.-M.; Nguyen, T. T.; Corwin, E. I.; Witten, T. A.; Jaeger, H. M. *Nat. Mater.* **2006**, *5*, 265.

(2) Nykypanchuk, D.; Maye, M. M.; van der Lelie, D.; Gang, O. *Nature* **2008**, *451*, 549.

(3) Redl, F. X.; Cho, K.-S.; Murray, C. B.; O'Brien, S. *Nature* **2003**, *423*, 968.

(4) Shevchenko, E. V.; Talapin, D. V.; Murray, C. B.; O'Brien, S. *J. Am. Chem. Soc.* **2006**, *128*, 3620.

(5) Evers, W. H.; Friedrich, H.; Filion, L.; Dijkstra, M.; Vanmaekelbergh, D. *Angew. Chem., Int. Ed.* **2009**, *48*, 9655.

(6) Dang, F.; Kato, K.; Imai, H.; Wada, S.; Haneda, H.; Kuwabara, M. *Cryst. Growth Des.* **2010**, *10*, 4537.

(7) Zhang, J.; Yang, H.; Yang, K.; Fang, J.; Zou, S.; Luo, Z.; Wang, H.; Bae, I.-T.; Jung, D. Y. *Adv. Funct. Mater.* **2010**, *20*, 3727.

(8) Demortière, A.; Launois, P.; Goubet, N.; Albouy, P.-A.; Petit, C. *J. Phys. Chem. B* **2008**, *112*, 14583.

(9) Quan, Z.; Fang, J. *Nano Today* **2010**, *5*, 390.

(10) Dang, F.; Mimura, K.; Kato, K.; Imai, H.; Wada, S.; Haneda, H.; Kuwabara, M. *Nanoscale* **2012**, *4*, 1344.

(11) Sun, S.; Murray, C. B.; Weller, D.; Folks, L.; Moser, A. *Science* **2000**, *287*, 1989.

(12) Yao, K. X.; Yin, X. M.; Wang, T. H.; Zeng, H. C. *J. Am. Chem. Soc.* **2010**, *132*, 6131.

(13) Shen, X. S.; Wang, G. Z.; Hong, X.; Zhu, W. *CrystEngComm* **2009**, *11*, 753.

(14) Wang, T.; Wang, X.; LaMontagne, D.; Wang, Z.; Wang, Z.; Cao, Y. C. *J. Am. Chem. Soc.* **2012**, *134*, 18225.

(15) Chen, C.-J.; Chiang, R.-K.; Jeng, Y.-R. *J. Phys. Chem. C* **2011**, *115*, 18142.

(16) Liao, C.-W.; Lin, Y.-S.; Chanda, K.; Song, Y.-F.; Huang, M. H. *J. Am. Chem. Soc.* **2013**, *135*, 2684.

(17) Yu, D.; Yam, V. W.-W. *J. Am. Chem. Soc.* **2004**, *126*, 13200.

(18) Wang, Y.; Zheng, Y.; Huang, C. Z.; Xia, Y. *J. Am. Chem. Soc.* **2013**, *135*, 1941.

(19) LaGrow, A. P.; Ingham, B.; Cheong, S.; Williams, G. V. M; Dotzler, C.; Toney, M. F.; Jefferson, D. A.; Corbos, E. C.; Bishop, P. T.; Cookson, J.; Tilley, R. D. *J. Am. Chem. Soc.* **2012**, *134*, 855.

(20) Dang, F.; Kato, K.; Imai, H.; Wada, S.; Haneda, H.; Kuwabara, M. *Cryst. Growth Des.* **2011**, *11*, 4129.

(21) Mimura, K.; Dang, F.; Kato, K.; Imai, H.; Wada, S.; Haneda, H.; Kuwabara, M. *Jpn. J. Appl. Phys.* **2011**, *50*, 09NC09.

(22) Yang, H.; Ogawa, T.; Hasegawa, D.; Takahashi, M. *J. Appl. Phys.* **2008**, *103*, 07D526.

(23) Malaquin, L.; Kraus, T.; Schmid, H.; Delamarche, E.; Wolf, H. *Langmuir* **2007**, *23*, 11513.

(24) Meijer, J.-M.; Hagemans, F.; Rossi, L.; Byelov, D. V.; Castillo, S. I. R.; Snigirev, A.; Snigireva, I.; Philipse, A. P.; Petukhov, A. V. *Langmuir* **2012**, *28*, 7631.

(25) Mimura, K.; Dang, F.; Kato, K.; Imai, H.; Wada, S.; Haneda, H.; Kuwabara, M. *Appl. Phys. Lett.* **2012**, *101*, 012901.

(26) Evers, W. H.; Goris, B.; Bals, S.; Casavola, M.; de Graaf, J.; van Roij, R.; Dijkstra, M.; Vanmaekelbergh, D. *Nano Lett.* **2013**, *13*, 2317.

(27) Li, M.; Schnablegger, H.; Mann, S. *Nature* **1999**, *402*, 393.

(28) Singh, A.; Gunning, R. D.; Sanyal, A.; Ryan, K. M. *Chem. Commun.* **2010**, *46*, 7193.

(29) An, K.; Lee, N.; Park, J.; Kim, S. C.; Hwang, Y.; Park, J.-G.; Kim, J.-Y.; Park, J.-H.; Han, M. J.; Yu, J.; Hyeon, T. *J. Am. Chem. Soc.* **2006**, *128*, 9753.

(30) Zhang, P.; Zhan, Y.; Cai, B.; Hao, C.; Wang, J.; Liu, C.; Meng, Z.; Yin, Z.; Chen, Q. *Nano Res.* **2010**, *3*, 235.

(31) Biswal, M.; Dhas, V. V.; Mate, V. R.; Banerjee, A.; Pachfule, P.; Agrawal, K. L.; Ogale, S. B.; Rode, C. V. *J. Phys. Chem. C* **2011**, *115*, 15440.

(32) Seo, W. S.; Jo, H. H.; Lee, K.; Kim, B.; Oh, S. J.; Park, J. T. *Angew. Chem., Int. Ed.* **2004**, *43*, 1115.

(33) Pan, J.; Sun, Y.; Wang, Z.; Wan, P.; Fan, M. *J. Alloys Compds.* **2009**, *470*, 75.

(34) Wang, J.; Du, N.; Wu, H.; Zhang, H.; Yu, J.; Yang, D. *J. Power Sources* **2013**, *222*, 32.

(35) Gao, J.; Lowe, M. A.; Abruna, H. D. *Chem. Mater.* **2011**, *23*, 3223.

(36) Wang, H.; Cui, L.-F.; Yang, Y.; Casalongue, H. S.; Robinson, J. T.; Liang, Y.; Cui, Y.; Dai, H. *J. Am. Chem. Soc.* **2010**, *132*, 13978.

(37) Wang, C.; Yin, L.; Xiang, D.; Qi, Y. *ACS Appl. Mater. Interfaces* **2012**, *4*, 1636.